

SOME OBSERVATIONS ON BUNCH LENGTHENING AT SPEAR*

M. A. Allen, G. E. Fischer, M. Matera, A. P. Sabersky, and P. B. Wilson

Stanford Linear Accelerator Center
Stanford University, Stanford, California 94305

I. Introduction

The phenomenon of current dependent bunch lengthening discovered at ACO and ADONE about seven years ago can be used as an engineering diagnostic tool to examine how the longitudinal electromagnetic field of a beam couples to its surroundings.¹ The importance of isolating such coupling factors is that they may give rise to damaging instabilities. Another practical reason for studying the effect is that if bunch lengths grow anomalously beyond those calculated on the basis of classical theory,² the effective luminosity of storage rings, particularly those employing low beta insertions, may be reduced.³ As in most other electron storage rings, the effect at SPEAR is observed to be large and may play a role in proton rings if the beam is highly bunched.

Two sets of theories explaining the effect exist. In one set it is suggested that the effect results from modification of the effective azimuthal potential well by beam loading. These theories can also lead to bunch shortening but not to an increase in the energy spread of the beam. A very general treatment, together with many examples of coupling impedance is put forth, for example, by Pellegrini and Sessler.⁴ The theoretical calculation of specific coupling impedances has received a great deal of attention in the last several years.⁵ On the other hand, an alternative explanation of bunch lengthening was advanced by Lebedev⁶ in which the effect arises due to instabilities of internal coherent synchrotron oscillations of the bunch. This concept has recently been extended to include the turbulent motion of the collective higher modes.⁷ The latter theories predict that the anomalous bunch lengthening is directly related to an increased energy spread of the beam. We believe that some ingredients from both sets of theories contribute.

In the following section we compare the functional dependence of the SPEAR bunch length with those of the various theories. In Section III the potential distortion model is used to extract a coupling impedance. The existence of coherent bunch shape oscillations is demonstrated in Section IV. Frequency shifts with current, and line widths are discussed. The excitation of theoretically predicted vacuum chamber modes is shown in the next section after which we estimate beam power absorption to those elements of the structure believed to cause bunch lengthening. In the final section, the prediction that the ferrite kicker magnet cores are presently the dominant elements is confirmed.

II. Bunch-Length Measurements and Data Reduction

The rms length σ_z of a single circulating bunch was measured as a function of wide-ranging values of average current I , total rf cavity voltage V_0 , and machine energy E_0 , by observing on a fast sampling oscilloscope the output from a specially mounted light-sensitive diode exposed to the optical part of the synchrotron-radiation spectrum. Details of this technique are reported elsewhere.⁸ A typical output scan is shown in Fig. 1. It is noted that at high currents the distribution tends to deviate from a purely Gaussian shape, and at times displays an asymmetric tail so that the values of σ_z calculated from the measured full width at half-maximum tend to lose their traditional meaning. (A discussion of bunch shape was recently presented by Haissinski.⁹) The data were corrected for instrumental rise time. The correction ranged from 30 percent at very low currents and very high voltages to an average of a few percent over most of the points taken.

*Work supported by the U. S. Atomic Energy Commission.

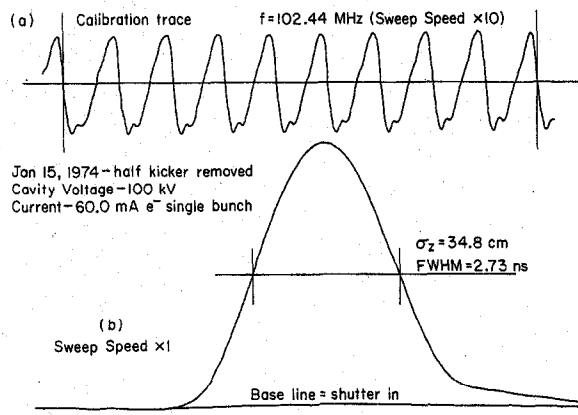


FIG. 1--A typical bunch length recording and calibration trace.

The so-called "natural bunch length" σ_{z0} , which results from the balance of quantum fluctuation and radiation-damping terms is calculated following the analysis of Sands² and is proportional to $E_0^{3/2} \alpha^{1/2} (V_0 \cos \phi)^{-1/2}$ and is of course independent of I . (Symbols used throughout this paper are identified in Table I.) The momentum compaction factor α and V_0 are singled out here because, in contrast to other machine parameters, they are not so well known and must be measured. Fortunately, the quantum lifetime near zero current, and the synchrotron frequency have a functional dependence on both α and V_0 and by a series of measurements of these quantities the cavity voltage readout was calibrated and α determined. The value of α found in this way differed from that calculated by the magnet-lattice program by only a few percent. Measurements taken over a span of one year with various different kinds of equipment reproduced to better than 10 percent.

Values of $R = (\sigma_z / \sigma_{z0})$ are plotted in Figs. 2, 3, and 4 as functions of I , E_0 , and V_0 , respectively. Some of the points shown in Fig. 2 were interpolated by less than 10% in

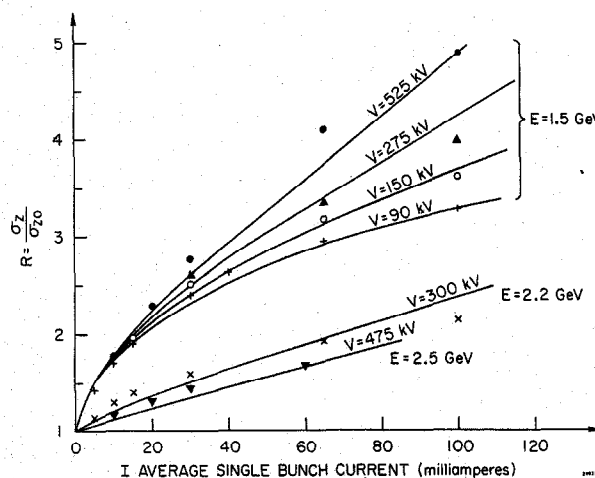


FIG. 2--The ratio $R = \sigma_z / \sigma_{z0}$ at various rf voltages and energies vs average single bunch current.

either current or voltage to facilitate intercomparison. For large R , the data demonstrate an $I^{1/3}$ dependence, which is also found at ACO¹⁰ and ADONE,¹¹ and which is common to

both sets of theories. For large I, the $E^{-5/3}$ dependence shown in Fig. 3 is also consistent with data from ACO and

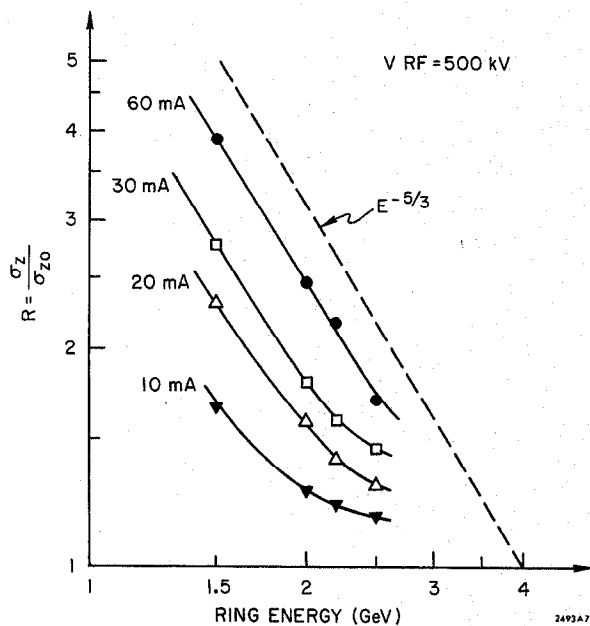


FIG. 3--R vs E_0 for various currents.

and ADONE. The potential distortion model⁴ predicts $E^{-3/2}$, the coherent synchrotron oscillation model $E^{-8/3}$ and the simplified turbulent higher-mode model⁷ $E^{-3/2}$. The dependence of R on cavity voltage is not so easily deciphered. Figure 4 shows that it is independent of voltage at very low

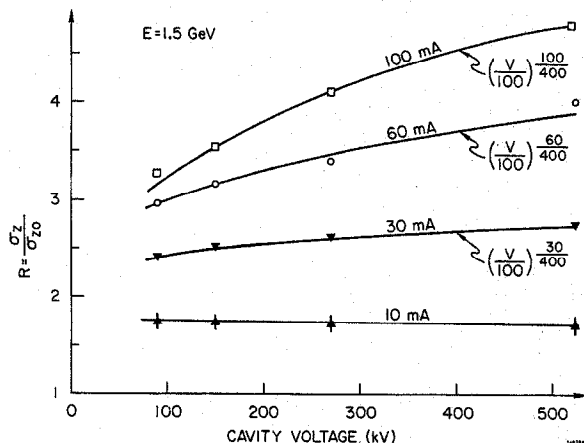


FIG. 4--R vs rf voltage at 1.5 GeV and various currents. The fit to the data indicates a power-law dependence on voltage, the exponent of which is proportional to current.

currents, but that it rises to as much as $V^{1/4}$ for higher currents. The ACO and ADONE results are fit approximately by $V^{1/6}$ while the existing theories predict $V^{1/6}$, $V^{1/2}$, $V^{1/6}$, respectively. From these considerations only, therefore, it is hard to distinguish between the various models.

To fit the data over a wide range of the ratio R, which must tend to 1 as the current approaches zero, the function

$$R = \frac{2}{\sqrt{3}} \cos(1/3 \arccos KI) \quad (1)$$

derived in Ref. 6 as formula (24) was chosen.

For large R, $R \approx (KI)^{1/3}$. A reasonable phenomenological fit to all SPEAR data is

$$KI = 0.92 I_{\text{mA}} \left(\frac{1.5}{E_{\text{GeV}}} \right)^5 \left(\frac{V_{\text{kV}}}{100} \right)^{\frac{3I_{\text{mA}}}{427}} \quad (2)$$

in which only the constant and the power of V were adjusted.

The solid lines drawn in Fig. 2 obtain from the formula for R shown above. Relevant machine parameters are listed in Table I.

TABLE I. SPEAR I Parameters

- r = average ring radius = 37.3 meters
- $\omega_0/2\pi$ = revolution frequency = 1.28 MHz
- ρ = magnetic radius = 12.7 meters
- α = momentum compaction factor = 0.04124 (configuration INJEQ)
- h = harmonic number = 40, rf frequency = 51.22 MHz
- j_ϵ = energy partition constant = 2
- τ_{rad} = synchrotron damping time at zero current = 33 msec at 1.5 GeV
- U = radiation loss per turn in kV
- Ω_0 = synchrotron frequency in kHz
- ϕ = synchronous phase angle in degrees
- σ_{ϵ_0} = rms energy spread at zero current in GeV
- σ_{z_0} = rms bunch length at zero current in cm
- R = the ratio σ_z/σ_{z_0}
- V_{rf} = total cavity voltage
- R = resistance

E_0 GeV	U kV	$\sigma_{\epsilon_0} \times 10^{-3}$	V_{rf} kV	ϕ degrees	Ω_0 kHz	σ_{z_0} cm
1.5	35	0.539	100	159	5.05	13.6
			300	173	9.03	7.6
			500	176	11.68	5.9
2.0	111	0.958	300	157	7.56	12.1
			500	167	10.00	9.2
2.5	270	1.49	500	147	8.2	13.8

III. Application of Bunch-Length Data

Two calculations have recently been performed using the previously published SPEAR data.¹² Sessler⁷ has found a surprisingly good fit using the turbulent mode model and finds a value of coupling impedance $Z_n = i46n$, where the integer n indicates the coupling frequency in multiples of the revolution frequency. However, the derived values of energy spread are about a factor of 3 larger than those actually found at SPEAR from measurements of the quantum lifetime of large current beams. Further attempts at measuring the energy spread are under way. Sacherer,¹³ on the other hand, applied the potential distortion model⁴ (no increased energy spread is contained in this theory) and found either $Z_n = i30n$, or $i360n^{1/2}$ to fit the data. He pointed out that this is much too large to be caused by the conductivity of the vacuum-chamber walls. More will be said on this point further on. It may be instructive to follow his analysis in a very simplified form.

Formula (2.8) of Ref. 4 relates the current dependent synchrotron frequency shift with bunch length as follows:

$$\left(\Omega^2 - \Omega_0^2\right) / \Omega_0^2 = 1 - \left(\frac{\sigma_z}{z}\right)^2 = 1 - \left(\frac{1}{R}\right)^2 \equiv x \quad (3)$$

In terms of an effective impedance Z_{eff} , x is also the ratio of the beam-induced voltage to the impressed voltage, i. e., $x = IZ_{\text{eff}}/hV_0 \cos \phi$.

In the case when Z_{eff} is dominated by the high frequency components of the beam one can write

$$Z_{\text{eff}} = i \sum_n n Z_n e^{-1/2 n^2 \sigma_z^2 \omega_0^2}$$

in which ω_0 is the revolution frequency for a single bunch machine and σ_z is in time units. If, for example, one assumes that Z_n is of a nonresonant form and can be fitted by a power law $Z_n = -iR |n|^s$, then the sum over n may be simply carried out and, for $s=1$, yields

$$Z_{\text{eff}} = \frac{2.5R}{(\sigma_z \omega_0)^3} \quad (4)$$

Substituting this in the above, we have

$$x = \frac{2.5R}{hV_0 \cos \phi \omega_0^3} \left(\frac{I}{\sigma_z^3}\right) \quad \text{or} \quad RI = \frac{x \sigma_z^3 V \cos \phi h \omega_0^3}{2.5} \quad (5)$$

For Eq. (3) one notes for large $R = \sigma_z / \sigma_{z0}$, x approaches 1 and from Eq. (5) the bunch length should then vary as $I^{1/3}$, consistent with observation. RI is plotted in Fig. 5, which

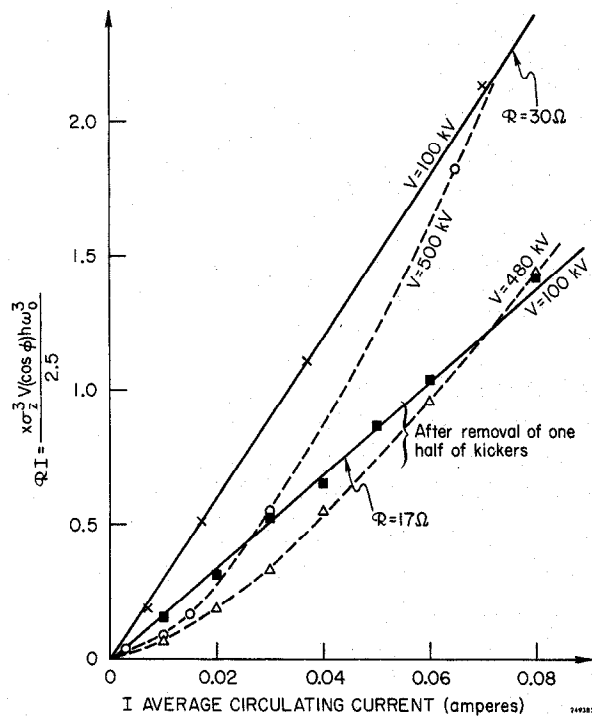


FIG. 5--The quantity $RI = \frac{x \sigma_z^3 V \cos \phi h \omega_0^3}{2.5}$ vs average current I .

demonstrates that a single value of $R = 30 \Omega$ fits the data quite well at low rf voltage so that simple assumption made about the form of Z_n is borne out. Data in the very short bunch regime, i. e., high voltage, low current regime, however, does not fit this simple model.

Several comments may be made at this point. First: Since σ_z is of the order of nanoseconds, very high harmonics of the revolution frequency are involved in the above sum and Z_{eff} is quite large, in fact, around 10^8 ohms, and one would expect the beam to lose a good deal of power somewhere around the ring. Second: Since x approaches 1, one would expect large shifts of the synchrotron frequency of particles in the bunch with current. These shifts will not be observed for the coherent center-of-mass motion or dipole frequency because the induced defocusing force of the beam on itself can be thought to be traveling around the ring with the bunch, but might be seen in the frequencies of high-order shape oscillations.^{6, 14}

IV. Observation of Coherent Bunch-Shape Oscillations

In summer of 1973, a high-gain low-frequency spectrum analyzer* was installed to permit more accurate measurement of betatron frequencies. This instrument can also be used to measure the frequencies of synchrotron oscillations, either those occurring naturally or those excited by frequency-modulating one main rf cavity driver. Again, the details of technique are reported elsewhere.⁸ Under certain operating conditions, especially for low cavity voltage and high beam current, a rich spectrum of naturally occurring lines was observed. Typical sweep traces are shown in Fig. 6. The

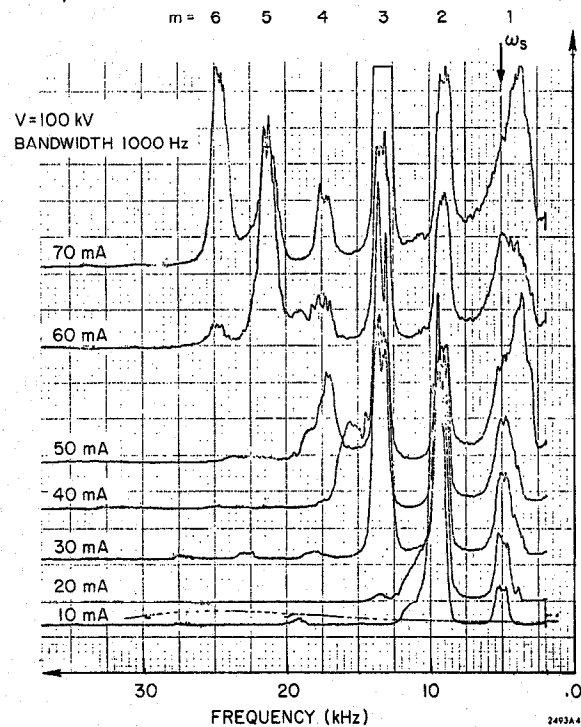


FIG. 6--Higher mode frequency spectrum tracings taken at 1.5 GeV, $V_{\text{rf}} = 100$ kV, and various currents.

frequencies of the lines seen are proportional to $(V \cos \phi)^{1/2}$ and arise from high-mode synchrotron oscillations. The current dependence of the frequencies is shown in Fig. 7. One may note that the shifts, down from integral multiples of the dipole synchrotron frequency, vanish at zero current. Also, at higher currents the frequency shifts become constant. We do not believe that the coherent dipole frequency shifts significantly with current at current levels below 60 mA.

During these measurements the cavity gap voltage was stabilized to compensate for beam loading.¹⁵

*Hewlett Packard Model 3950A.

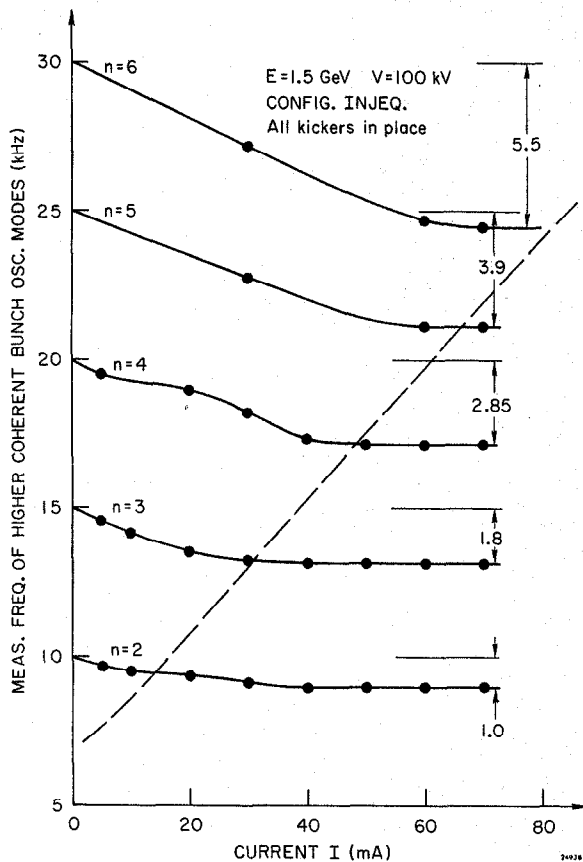


FIG. 7--Higher mode frequencies vs single bunch average current. The shifts from multiples of the synchrotron frequency are indicated on the right in kHz.

Further demonstration that the lines arise from shape oscillation stems from the following experiment. One main rf cavity was externally phase-modulated at the shifted frequency $\Omega_Q = 2\Omega_s - \Delta\Omega$ and the bunch shape was photographed using the sampling oscilloscope with its trigger locked to the modulating frequency. A series of photographs taken at various fixed times in the modulating cycle therefore represent a slow motion sequence of the oscillation and clearly showed the "breathing" nature of the quadrupole mode. Under certain conditions of cavity voltage and beam current, specific naturally occurring modes become dominant. A multiple trace photograph of a bunch executing sextupole oscillations is shown in Fig. 8. This shape is precisely that

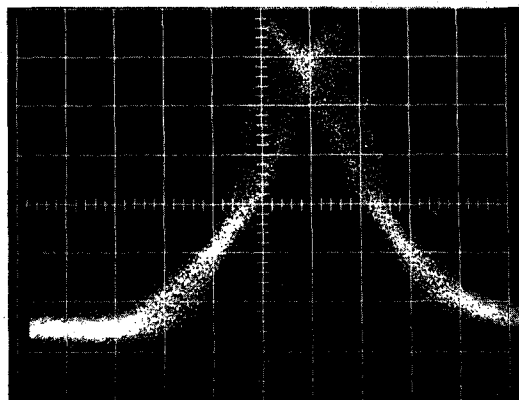


FIG. 8--Multiple sweep photograph of sampling oscilloscope showing self-excited

coherent sextupole oscillations of the bunch shape. Sweep speed=1 nsec/cm. Single bunch e^- current 134 mA at 1.5 GeV. Cavity voltage 235 kV.

outlined by Sacherer (Fig. 1, $m=3$ in Ref. 14). The octupole mode could also be seen in this way.

We turn now to the magnitude of the frequency shifts as a function of mode number m . The convention used is: For the dipole, $m=1$, quadrupole, $m=2$, etc. The importance of examining this dependence is that various impedance structures would yield differing results.¹⁴ Examining Fig. 7, one sees that the frequency shifts do not bear a fixed relationship to each other until high currents are reached. Something more complicated must be going on. In spite of this, the higher mode frequencies at large current are well fitted by expression (45) of Ref. 18, $\omega_{mn} = nQ_z + 2nC_{mn}\Delta Q$ in which $Q_z = Q_{z0} - \Delta Q$ and we have set $m=n$ for the fastest growing modes. The coefficients C_{mn} used were those calculated by Sacherer for the so-called Legendre modes that arise from a parabolic charge distribution. From the fit, one finds $\Delta Q = 0.83$ kHz at $Q_z = 5.0$ kHz. Since $C_{11} = 0.5$ the dipole frequency does not shift with current in this theory.

As stated before, specific modes are preferentially excited at certain currents. In fact, this is observed to occur for those currents at which the dashed line in Fig. 7 intersects the frequency of that mode. Even harder to understand is the appearance in the spectra of a relatively broad line, whose frequency is given by this dashed line. The first observation might be explained as follows. Suppose there exists in the ring a beam-excited resonant gap of spacing $D = \lambda/2$, so that when the total bunch length $4\sigma_z = m\lambda/2$, the m th mode is preferentially coupled. This picture corresponds to the form-factor treatment of Ref. 14. Unfortunately the predicted even spacing in bunch length with m is not borne out. The second observation suggests that there exists inside the bunch a separate population of particles, which oscillate coherently at frequencies linearly proportional to the total current and when frequencies coincide, preferential mode excitation occurs. Although the observed modes are clearly coherent, it is not yet possible to tell precisely what fraction of the bunch population is oscillating coherently.

The above discussion concerns the real part of the frequency shift. A measure of the imaginary part was obtained in two ways: swept line widths and decoherence times following shock excitation. The techniques are reported elsewhere⁸ and were first tried out on the dipole line. Near zero current, this line displays a proper Lorentzian shape and yields the proper classical damping time. Both cavity detuning, producing Robinson¹⁶ damping and phase feedback (when used),¹⁵ broaden the line correctly. Both instrumental methods give the same results. Although rf-system damping should be different for the quadrupole mode, the observed line shape, taken with high resolution, is not understood. Moreover, the full width at the base is too narrow to fit the generally accepted stability criterion¹⁴ that the spread be greater than the shift. This last fact may, however, be consistent if mode mixing, suggested in the turbulent equilibrium theory,¹⁷ contributes. At the highest operating energies (2.5 GeV) quantum fluctuations appear to wash out the coherent modes.

V. Observation of Vacuum-Chamber Resonances

In SPEAR, the aluminum-extruded, curved vacuum chambers that thread through the bending magnets are connected to each other by round, 2-meter long 20-cm-diameter stainless-steel tubes. The tubes house a variety of machine elements. Common to each straight section is a subsection containing a set of beam position pickup electrode buttons. Signals from these electrodes were observed to contain very

high frequency components which were found not to be characteristic of the electrodes and their associated circuitry.¹⁹ A detailed spectrum-analyzer examination of all twenty stations showed lines at 1.1, 1.4, and 1.8 GHz (Fig. 9). These

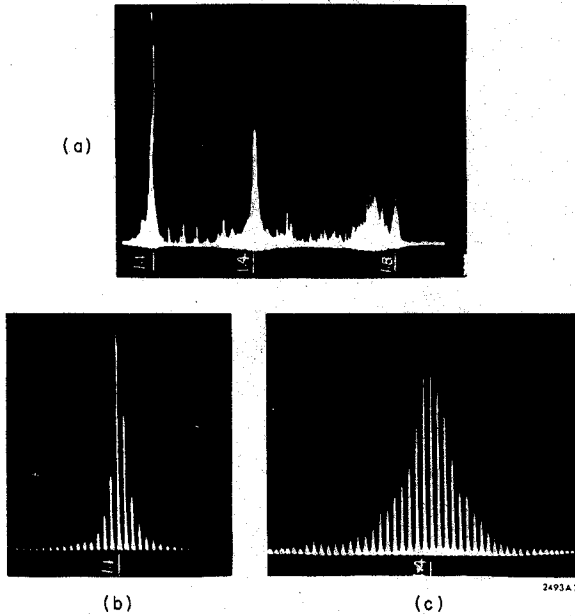


FIG. 9--Spectrum analyzer traces showing resonances in cylindrical vacuum-chamber straight sections at 1.1, 1.4, and 1.8 GHz. (a) 100 MHz/cm, (b) and (c) expanded scales showing lines which are high harmonics of the 1.28 MHz revolution frequency. The ordinates are proportional to power. Taken at 20 mA, 1.5 GeV, 500 kV.

frequencies are just those of the so-called "waveguide modes," which are independent of cavity length and are mentioned in Ref. 4. Their usual designation is TM_{010} , TE_{210} ($TM_{110} - TE_{010}$), respectively. Transverse magnetic modes certainly could be excited by the axial electric field of the beam, and the cavity impedance for these modes can be estimated. In fact, one of the first calculations explaining bunch lengthening correctly was due to Robinson²⁰ who considered the fields due to vacuum chamber discontinuities. For the TM_{010} mode for example, one has the relation,

$$\frac{R}{Q} = 308 \sin(\pi l/\lambda) \quad (5)$$

where l is the length of the cavity and λ the resonant wavelength. The Q of the 1.1 GHz mode is estimated from Fig. 9 to be about 400. For twenty elements having a length $l \sim \lambda/2$, the preceding relation then gives a total impedance of about 2.5×10^6 ohms, a significant value.

Since the purpose of this investigation is to attempt to determine which machine elements couple strongly to the beam, further miscellaneous tests were performed. The electric separation plates (normally terminated) and the electric quadrupole conductors were shorted to ground or opened. The 3rd harmonic cavity¹⁵ shorting bar was removed. The tuning paddle in an idling rf cavity was moved to resonance. None of these impedance changes affected the bunch length measurably.

VI. Beam-Power-Loss Estimates

A. Kicker Magnets

Following Sacherer,¹³ one may write for the power dissipation

$$P = \frac{1}{2} I^2 \sum_n \text{Re } Z_n e^{-n^2 \sigma_z^2 \omega_0^2} \quad (6)$$

Assuming the resistive part of Z_n to be of the same order as the reactive part, i. e., $\text{Re } Z_n = \mathcal{R} |n|$, substituting, and performing the sum gives

$$P = \frac{1}{2} \frac{I^2 \mathcal{R}}{(\sigma_z \omega_0)^2} \quad (7)$$

For a beam current of 50 mA and using the value of \mathcal{R} obtained from the fits in Fig. 5, one finds a loss of between 400 and 800 watts, the higher figure obtained from shorter bunches obtained with higher cavity voltages. The elements most likely to be responsible for this loss are the ferrite-kicker magnet cores which have been observed to have a large thermal outgassing rate, not associated with synchrotron radiation, in the presence of high current beams. The power dissipated per unit volume in the ferrite core at frequency ω is

$$P(\omega)/v = \frac{1}{2} \omega \mu'' \mu_0 H^2(\omega) \quad (8)$$

in which μ'' is related to the loss tangent and relative permeability by $(\mu''/\mu_r) = \tan \delta$. Using values of μ'' and μ_r for the 4C4 Ferroxcube material found in the literature,^{21, 22} one can perform the sum over the high-frequency components of the beams numerically and find a power loss of about 100 watts for each of the four kickers, the loss peaking very broadly at frequencies of about 100 MHz. Unfortunately, it is not known exactly what material the manufacturer actually provided, so this rather good agreement is only qualitative but is consistent with core heating times.

B. Cavity Modes

An estimate of power loss to the cylindrical cavity modes can also be made. In this case, one is dealing with low- Q resonators at specific high frequencies. The excitation of, for example, the 1.1 GHz TM_{010} mode depends strongly on bunch lengths, which in turn is a function of current. The total beam loading voltage due to all twenty resonators can be written

$$V_T = I R_T f_1(\sigma_z) f_2(T_0/T_F) \quad (9)$$

where $f_1 = e^{-\omega^2 \sigma_z^2 / 2c^2}$ gives the component of the current at frequency ω resulting from the finite bunch length. The function f_2 gives the enhancement in the energy loss which results when the bunch revolution time, T_0 becomes comparable to the decay time, T_F , for the mode in question. For SPEAR, T_0 is 0.78 μsec , for a cavity with a Q of 400 at 1.1 GHz, $T_F = 0.12 \mu\text{sec}$ giving $T_0/T_F = 6.6$. In Ref. 23 it is shown that for $T_0/T_F \gg 1$, $f_2 \sim 1/2 (T_0/T_F) = 3.3$. The function f_1 decreases rapidly with increasing current because of the increase in bunch length. The product $I f_1$, in fact, reaches a maximum value of 0.9 mA at a current $I = 5$ mA. Using $R_T = 2 \times 10^6$ ohms as previously calculated, V_T is about 6 kV. The total power dissipation is $I f_1 V_T = 5$ W. The power dissipated in all of the cavity modes might be several times this, or about 15 W. In contrast to the situation at DORIS,²⁴ resistive losses due to the aluminum vacuum chamber wall with these bunch lengths amount to no more than a few watts.

VII. Effect of Removing Half the Kicker-Magnet Core

In January, 1974, two of the four magnets were replaced with ferriteless magnets of a new design. Bunch lengths and frequency shifts were remeasured. The results are shown best in Fig. 5. If the ferrite cores were the dominant bunch-lengthening component and half of them were removed from the ring, one should expect the slope of $\mathcal{R}I$ to be halved. This is indeed nearly the case. For higher voltages, i.e., short bunches, the effect is less dramatic. The resultant ~20 percent reduction in bunch length (recall Eq. (5)) also shows up in the mode spectra. The rich spectrum up to 6th order previously seen at 70 mA now contains prominent lines only up to order 2, but can be reproduced at 170 mA. The frequency shifts of the higher modes are also uniformly reduced by 25 percent. Removal of the remaining two kicker cores is scheduled for May, 1974, at which time large further reduction of bunch length is expected. How close to the theoretical value it becomes will depend then on the influence of the aluminum-chamber impedance, cavity-mode excitation, and as yet unidentified elements whose effects have been masked by those of the kickers. Further, an entirely new regime will obtain after conversion of SPEAR to higher energies. The present RF system will be replaced with one of seven times the frequency and capable of providing accelerating voltages up to 7 MeV/turn. The resulting extremely high peak currents of a single bunch will no doubt raise interesting new problems.

VIII. Conclusions

On the basis of the data obtained at SPEAR, ACO, and ADONE, we conclude that no single theory presently explains the bunch lengthening effect, however, use of existing theories has lead us to identify the dominant element responsible in SPEAR. The search for other elements will continue after all the ferrite kicker magnet cores have been removed. We find that the existence of higher order bunch-shape oscillations, and measurements of their real and imaginary frequency shifts provide an additional, perhaps simpler tool for the study of the electromagnetic beam-environment interaction. It remains to compare such observations with theory in a quantitative way.

Acknowledgments

We wish to thank the other members of the SPEAR Group, R. Helm, M. Lee, P. Morton, J. M. Paterson, B. Richter, and the operating staff for their assistance.

References

1. A. M. Sessler, IEEE Trans. Nucl. Sci. NS-18 (1971) 1039.
2. M. Sands, Physics with Intersecting Storage Rings, ed. by B. Touschek (Academic Press, New York, 1971), p. 257 or Report No. SLAC-121, p. 129, Stanford Linear Accelerator Center (1970).
3. G. Fischer, SPEAR-154 (internal note), Stanford Linear Accelerator Center (1973); E. Keil, CERN/ISR-TH/72-33.
4. C. Pellegrini and A. M. Sessler, Nuovo Cimento 3A (1971) 116.
5. For examples, see references listed in 1, above.
6. A. N. Lebedev, Physics with Intersecting Storage Rings, loc. cit., p. 184.
7. A. M. Sessler, PEP Note 28, Lawrence Berkeley Laboratory (April 1973) (unpublished).
8. A. P. Sabersky, these proceedings.
9. J. Haissinski, Nuovo Cimento 18B (1973) 72.
10. R. Belbeoch et al., Proceedings of the National Conference on Particle Accelerators No. 1, Moscow, USSR, 1968; p. 129.
11. F. Amman, Proceedings VIIIth International Conference on Accelerators, CERN, Geneva, 1971; p. 68.
12. B. Richter et al., IEEE Trans. Nucl. Sci. NS-20 (1973) 755.
13. F. Sacherer, PEP Summer Study Note No. 45 (August, 1973).
14. F. Sacherer, IEEE Trans. Nucl. Sci. NS-20 (1973) 825.
15. M. A. Allen, R. A. McConnell, IEEE Trans. Nucl. Sci. NS-20 (1973) 373.
16. K. Robinson, CEAL 1010 (1964) unpublished.
17. A. M. Sessler, IEEE Trans. Nucl. Sci. NS-20 (1973) 856.
18. F. Sacherer, CERN/SI-BR/72-5, unpublished.
19. W. Dumond, R. Melen, M. Matera, SPEAR-168 (internal note), Stanford Linear Accelerator Center (1973).
20. K. Robinson, CEAL-TM-183 (July 1969) unpublished.
21. H. P. J. Wijn et al., Rev. Mod. Phys. 25 (1953) 91.
22. F. G. Brockman et al., Philips Technical Review 30 (1969) 324.
23. P. B. Wilson, PEP Note 37, SPEAR-163 (internal note), Stanford Linear Accelerator Center (1973).
24. A. Piwinski, DESY Report 72/72 (December, 1972).